Nanoscale

ROYAL SOCIETY OF CHEMISTRY

PAPER

View Article Online
View Journal | View Issue

Cite this: *Nanoscale*, 2023, **15**, 14423

In vitro assessment of skin irritation and corrosion properties of graphene-related materials on a 3D epidermis†

Michela Carlin, [a] Marina Garrido,[b,c] Silvio Sosa,[a] Aurelia Tubaro, [a] Maurizio Prato [b,d,e] and Marco Pelin *[a]

The increasing use of graphene-related materials (GRMs) in many technological applications, ranging from electronics to biomedicine, needs a careful evaluation of their impact on human health. Skin contact can be considered one of the most relevant exposure routes to GRMs. Hence, this study is focused on two main adverse outcomes at the skin level, irritation and corrosion, assessed following two specific Test Guidelines (TGs) defined by the Organization for Economic Co-operation and Development (OECD) (439 and 431, respectively) that use an *in vitro* 3D reconstructed human epidermis (RhE) model. After the evaluation of their suitability to test a large panel of powdered GRMs, it was found that the latter were not irritants or corrosive. Only GRMs prepared with irritant surfactants, not sufficiently removed, reduced RhE viability at levels lower than those predicting skin irritation (≤50%, after 42 min exposure followed by 42 h recovery), but not at levels lower than those predicting corrosion (<50%, after 3 min exposure or <15% after 1 h exposure). As an additional readout, a hierarchical clustering analysis on a panel of inflammatory mediators (interleukins: IL-1α, IL-1β, IL-6, and IL-18; tumor necrosis factor-α and prostaglandin E_2) released by RhE exposed to these materials supported the lack of irritant and pro-inflammatory properties. Overall, these results demonstrate that both TGs are useful in assessing GRMs for their irritant or corrosion potential, and that the tested materials did not cause these adverse effects at the skin level. Only GRMs prepared using toxic surfactants, not adequately removed, turned out to be skin irritants.

Received 26th June 2023,
Accepted 9th August 2023

DOI: 10.1039/d3nr03081d

rsc.li/nanoscale

Introduction

In the last few years, the development of new nanomaterials and nanotechnologies has widely increased. Due to their unique physical and chemical properties, carbon-based materials (CBMs), and in particular graphene-related materials (GRMs), can be integrated into a large number of application areas, including electronics, biomedical technologies, energy storage, composites, coatings, and water and wastewater treatments.[1] The use of these materials is so promising that market forecasts predict the global graphene market size to reach 1.6 billion dollars within 2028, with respect to 125.7 million dollars of 2021.[2]

Until a few years ago, the risk for human health associated with GRMs was mainly correlated with occupational settings, during their industrial or small-scale production. In this scenario, skin exposure and inhalation can be considered the most feasible exposure routes to GRMs for workers.[3] However, *Graphene Market, Production and Pricing Report 2022* states a remarkable market increase in commercial graphene collaborations, agreements, investments and, most importantly, product launches.[4] Especially considering the latter, European Union (EU) companies need to comply with the EU regulation on registration, evaluation, authorisation, and restriction of chemicals (REACH), applied to chemical substances produced and/or imported for a total amount higher than 1 ton per year. According to REACH regulation, a registration dossier for graphene is currently present at the European Chemical Agency (ECHA), even though with limited toxicological data.[5] Considering the REACH regulation, toxicological data should be collected following robust, reliable, predictive and accurate toxicity studies.[6] In this context, an important role is established by validated test guidelines (TGs) for safety evaluation,

[a]*Department of Life Sciences, University of Trieste, Via Fleming 22, 34127 Trieste, Italy. E-mail: mpelin@units.it; Tel: +39 040 5588620*
[b]*Department of Chemical and Pharmaceutical Sciences, University of Trieste, Via Giorgieri 1, 34127 Trieste, Italy*
[c]*IMDEA Nanociencia, C/Faraday 9, Ciudad Universitaria de Cantoblanco, 28049 Madrid, Spain*
[d]*Center for Cooperative Research in Biomaterials (CIC biomaGUNE), Basque Research and Technology Alliance (BRTA), San Sebastián, 20014, Spain*
[e]*Basque Foundation for Science (IKERBASQUE), Bilbao, 48013, Spain*

† Electronic supplementary information (ESI) available. See DOI: https://doi.org/10.1039/d3nr03081d

such as those given by the Organization for Economic Co-operation and Development (OECD) and the International Organization for Standardization (ISO). Examples may be presented by the ISO/TC 229 Nanotechnologies and the OECD Guidelines for the Testing of Chemicals, a series of commonly accepted procedures that should be rigorously followed to identify and characterize hazards from chemical substances, suitable also for regulatory purposes.

In general, cutaneous exposure can be considered one of the most relevant exposure routes for GRMs.[7] Due to its anatomical structure, human skin, and in particular its outermost layer epidermis, plays an important role as a barrier, since it forms the first line of defence with repeated exposure to physical, chemical and biological external agents. On top of that, several studies define GRMs as useful nanotools for a wide range of applications, including those involving a possible skin exposure, such as flexible electronics, smart textiles, wound healing dressing, electronic skin, skin sensors and drug delivery systems.[8–11] Given the importance of skin exposure to GRMs, some *in vitro* studies on the effects of different GRMs towards fibroblasts and keratinocytes are available.[12–20] It was demonstrated that few layer graphene (FLG) and graphene oxide (GO), after a strong and only partially reversible interaction with the cell membrane,[17] reduced HaCaT keratinocyte viability with an effect depending on their oxidation state and, secondly, on their lateral dimensions.[12] These materials caused a reactive oxygen species (ROS)-dependent mitochondrial dysfunction[13,15,18] by the activation of flavon-based oxidative enzymes,[13] with a consequent rearrangement of the keratinocyte metabolome.[15,19] Moreover, exposure of HaCaT cells to graphene nanoplatelets (GNP) for 12 and 24 h induced a time-dependent cytotoxicity, with a proliferative activity at non-cytotoxic concentrations.[16] Subsequent studies showed that endotoxin-free FLG and thermally dehydrated GO (d-GO) trigger a pro-inflammatory response in skin keratinocytes by inducing the release of cytokines (*e.g.*, IL-1α, IL-6, IL-8 and TNF-α), particularly under recovery conditions (4 h exposure, followed by 20 or 64 h incubation without the materials).[21] However, these materials were unable to further modulate monocyte differentiation and migration, a result arguing against a sensitization potential. In this view, skin sensitization properties have been recently excluded for different GRMs both by *in vitro* (GNP)[22] and *in vivo* studies (GNP, FLG and GO)[22,23] carried out following specific OECD guidelines.

Considering the need for robust toxicological data on the cutaneous effects of GRMs, in this study we focused on two main adverse outcomes at the skin level (irritation and corrosion), following two specific OECD TGs (439 and 431, respectively) that use an *in vitro* model constituted by the three-dimensional (3D) reconstructed human epidermis. This epidermal model, characterized by a tissue morphology similar to that of human epidermis, provides toxicological data suitable to characterize the hazard at the skin level, avoiding the use of animals.[24] Regarding skin irritation, a preliminary study was already published by our group, focusing on a limited panel of GRMs.[25] In the present follow-up study, the panel of GRMs has been widened, investigating not only their irritant, but also their corrosive, potential. The study includes also other related nanomaterials, such as multi-walled carbon nanotubes (MWCNTs) and carbon black (CB) as reference carbon-based materials (CBMs). In addition, being originally validated for chemicals, OECD TGs were carefully characterized for these materials, considering different parameters, to exclude any bias due to technical issues, limiting the possible adoption of these guidelines for GRMs.

Materials and methods

Materials

GNP (GNP Grade 4) was purchased from CheapTube (Grafton, USA), whereas GO (Batch #DGOP21001) and reduced GO (rGO; batch #rGOP20006) were kindly provided by Graphenea S.A. (San Sebastian, Spain). Their complete physico-chemical characterization was previously reported.[25] Regarding CBMs, carbon black (CB) was purchased from Sigma-Aldrich (Milan, Italy; product code 699632; CAS 1333-86-4), whereas multi-wall carbon nanotubes (MWCNTs) were purchased from Nanoamor (Katy, USA; stock # 1237YJS, 95%, OD 20/30 nm, length 0.5–2 μm) and Nanocyl (Sambreville, Belgium; 7000 series, lot number MWM P031105, 90%, average diameter: 9.5 nm, average length: 1.5 μm). All the other reagents, if not otherwise stated, were purchased from Sigma-Aldrich (Milan, Italy).

Synthesis of GRMs

Sodium dodecyl sulfate (SDS)-exfoliated few-layer graphene (FLG-SDS). Washed and non-washed FLG-SDS samples were prepared as previously described.[25] Briefly, graphite (1 g) was added to 200 mL SDS/Milli-Q water solution (0.05 mg mL^{-1}). The dispersion was then sonicated for 2 h and subsequently centrifuged for 45 min at 500 rpm. Finally, the supernatant was collected and lyophilized, affording the final non-washed FLG-SDS powder. Washed FLG-SDS was prepared in the same manner, but the supernatant was filtered and cleaned with Milli-Q water several times, in order to remove SDS residues.

Research-grade graphene oxide (GO). GO was prepared using a modified Hummers' method.[26] Graphite (3 g) and $NaNO_3$ (1.5 g) were dry-mixed in a 500 mL round bottom flask. Then H_2SO_4 (conc. 69 mL) was added, and the mixture was stirred at 0 °C on an ice bath. When the powder was fully dispersed, $KMnO_4$ (9 g) was added slowly to the suspension. The addition rate was carefully controlled to keep the temperature below 20 °C. After the addition was completed, the suspension was stirred at 0 °C for an additional 10 min. The reaction mixture was warmed to 35 °C and stirred for 30 min. Afterward, water (138 mL) was added slowly, producing a large exotherm at 98 °C. External heating was introduced to maintain the reaction temperature at 98 °C for 15 min. Then, the heat was removed, and the reaction mixture was cooled using a water bath for 10 min. Additional water (420 mL) and 30% H_2O_2 (10 mL) were added, producing other exotherms. The

reaction mixture was cooled to room temperature and the brown suspension was filtered under vacuum on a PTFE membrane and dried for 24 h at 80 °C. The solid obtained (4.12 g) was divided into three fractions to prepare three kinds of GO with different cleaning degrees (non-clean GO, HCl-clean GO and clean-GO).

Non-clean GO. One fraction of the previous three samples was employed without further purification for the exfoliation step. GO (500 mg) was suspended in 200 mL of Milli-Q water, sonicated for 2 h and subsequently centrifuged for 45 min at 500 rpm. Finally, the supernatant was collected and lyophilized, affording the final non-clean GO powder.

HCl-clean GO. The remaining initial two fractions were redispersed in 200 mL of 1 M HCl, sonicated for 10 min, filtered under vacuum on a PTFE membrane and cleaned with additional 1 M HCl until the collected filtrate solution became nearly transparent. The obtained solid was dried for 24 h at 80 °C and then divided into two fractions. One of these fractions was employed for the exfoliation step. The exfoliation procedure is the one described for non-clean GO. After the lyophilization, HCl-clean powder was obtained.

Clean GO. The remaining fraction was dispersed in 200 mL warm Milli-Q water, sonicated for 10 min, filtered under vacuum on a PTFE membrane and cleaned with additional warm Milli-Q water until the pH was neutralized. The obtained solid was dried for 24 h at 80 °C. The obtained powder was employed for the exfoliation step, similar to the other fractions. After the lyophilization, clean GO powder was obtained.

Characterization techniques

Raman spectra were recorded on a Renishaw inVia Raman Microscope at room temperature using an exciting laser source of 532 nm. Raman samples were measured in the solid state under ambient conditions. Transmission electron microscopy (TEM) micrographs were obtained using a Philips EM208 TEM and RADIUS 2.0 software (EMSIS GmbH, Muenster, Germany). The samples were dispersed in Milli-Q water and dropped onto a lacey carbon copper grid (300 mesh); the solvent was removed at room temperature. Thermogravimetric analyses (TGA) were performed with a TGA Q500 (TA Instruments) under a N_2 atmosphere. The sample was introduced inside a platinum crucible and equilibrated at 100 °C followed by a 10 °C min^{-1} ramp between 100 and 800 °C. Elemental analyses (CHNS) were performed with a Flash 2000 Thermo Scientific Analyzer. X-ray diffraction (XRD) analyses were performed with a Bruker D8 diffractometer equipped with a Göbel mirror and a CuKα X-ray source (λ = 1.5418 Å). ICP/MS analyses were performed with an iCAP-Q ICP-MS equipment (Thermo Scientific, Bremen, Germany) equipped with an autosampler ASX-500 (CETAC Technologies, Omaha, USA).

SkinEthic™ reconstructed human epidermis model

The SkinEthic™ reconstructed human epidermis (RhE) model is a completely differentiated 3D epidermal tissue composed of normal human keratinocytes cultured at the air–liquid interface on an inert polycarbonate filter, grown in a chemically defined medium. This model is histologically similar to normal human epidermis. The SkinEthic™ RhE was purchased from Episkin (Lyon, France) and produced under ISO9001 certification. Every batch of RhE was accompanied by a quality control data sheet including data on histology, morphology, cell viability, barrier function integrity and tissue safety.

Skin irritation

Skin irritation induced by GRMs, and CBMs as reference materials, was assessed on the SkinEthic™ RhE model following OECD Test Guideline (TG) no. 439.[27] Before using RhE tissues, technical proficiency was assessed[25] testing ten Proficiency Chemicals, according to OECD TG 439. Considering the OECD TG acceptability parameters, quality control criteria were met (ESI Table T1†).

As indicated in the OECD TG 439, RhE tissues (0.5 cm^2, day 17) were incubated in 6-well plates containing 1 mL growth culture medium for 2 h at 37 °C, 5% CO_2 and 95% humidity. Afterwards, 10 μL distilled H_2O were added to RhE tissue before its exposure for 42 min to 16 mg of each GRM or CBM (32 mg cm^{-2}), in duplicate. As negative and positive controls, RhE was exposed to 16 μL phosphate buffered saline (PBS) or 5% sodium dodecyl sulfate (SDS) solution, respectively. The tissues were then washed thoroughly 25 times with 1 mL PBS and transferred into a 6-well plate containing 2 mL growth culture medium for 42 h post-treatment incubation at 37 °C, 5% CO_2 and 95% humidity. Subsequently, the inserts were transferred into a 24-well plate containing 300 μL of methylthiazolyldiphenyl-tetrazolium bromide (MTT; 1 mg mL^{-1}) solution. The plate was then incubated for 3 h at 37 °C, 5% CO_2 and 95% humidity. Formazan salts were then extracted from both the top and bottom sides of each tissue insert with 1.5 mL isopropanol, for 2 h under gentle shaking at room temperature (RT). The tissues were than perforated and the formazan extract was homogenized. For each tissue, 200 μL of this solution were transferred into each well of a 96-well plate, in triplicate; isopropanol was used as a blank. Tissue viability was evaluated in terms of formazan concentration, measuring the optical density (OD) of each extract at 570 nm using the FLUOstar® Omega microplate reader (BMG LABTECH; Ortenberg, Germany). After subtracting the blank OD from all raw data, the mean OD and standard error were calculated. The results of tissue viability are reported as % of negative controls (vehicle) and are the mean ± standard error (SE) of three independent experiments. As a threshold given by OECD TG 439, tissue viabilities ≤50% define a substance as an irritant.

As preliminary analysis, the possible interference between nanomaterials and MTT was investigated. To identify if GRMs and CBMs were direct MTT reducers, each material was added to freshly prepared MTT solution (1 mg mL^{-1}) for 3 h. An additional check employed killed tissues to evaluate non-specific reduction of MTT. As reported in the OECD TG 439, killed RhE tissues were obtained by freezing RhE at −80 °C for 48 h and further processed for GRM and CBM treatment and MTT assay as reported above. None of the materials showed

any non-specific color interferences and non-specific MTT reduction.

Before the use of OECD TG 439, to assess the irritation potential of the selected GRMs, two critical parameters were considered to evaluate its possible adoption for GRMs: (i) the final readout, since GRMs may interfere with the OD measurement of the MTT-derived formazan[28] and (ii) the materials concentrations to be tested since, volumetrically speaking, 32 mg cm^{-2} represents a too big concentration for GRMs, considering their lightweight nature. Regarding the first point, the 2-(2-methoxy-4-nitrophenyl)-3-(4-nitrophenyl)-5-(2,4-disulfophenyl)-2*H*-tetrazolium (WST-8) assay was proposed in place of the MTT assay, since WST-8 does not seem to suffer from any unspecific interference with GRMs.[28] After RhE treatment (42 min + 42 h post-treatment incubation), the inserts were transferred into each well of a 24-well plate containing 270 μL maintenance culture medium with 30 μL of WST-8. The plate was then incubated for 3 h at 37 °C, 5% CO_2 and 95% humidity. For each tissue, 100 μL of this solution were transferred into each well of a 96-well plate, in triplicate, and tissue viability was quantified by measuring the OD at 450 nm using a FLUOstar® Omega microplate reader (BMG LABTECH, Ortenberg, Germany). The results of tissue viability are reported as % of negative controls (vehicle) and are the mean ± SE of three independent experiments.

Considering the second parameter, the procedure described by the OECD TG 439 was applied using lower GRM concentrations (0.5–2.0–8.0 mg cm^{-2}) in addition to that stated in the TG (32.0 mg cm^{-2}).

Release of inflammatory mediators

To evaluate the pro-inflammatory response by GRM- or CBM-exposed RhE, tissue media were rapidly and directly collected after RhE treatment (42 min exposure with nanomaterials or controls, followed by 42 h post-treatment incubation), and stored at −80 °C. A panel of inflammatory mediators, including interleukin (IL)-1α, −1β, −6, −8, and −18, tumour necrosis factor (TNF)-α and prostaglandin E_2 (PGE_2), was quantified by a sandwich or competitive ELISA from Diaclone (Besançon, France) or Elabscience (Bologna, Italy) following the manufacturers' instructions. The concentration of each inflammatory mediator in tissue media (pg mL^{-1}) is the mean ± SE of three independent experiments. A heatmap was used to visualize the pattern of inflammatory mediators' release induced by different nanomaterials and a hierarchical clustering analysis between the different samples was performed.

Skin corrosion

Skin corrosion induced by GRMs and CBMs was assessed on the SkinEthic™ RhE model following the OECD Test Guideline (TG) no. 431.[29] Before using RhE tissues, quality control criteria were checked (ESI Table T1†) and technical proficiency was assessed testing twelve reference Proficiency Substances, according to OECD TG 431.

Similar to what has been previously reported for skin irritation (OECD TG 439), the possible interference between nanomaterials and MTT was excluded by preliminary analysis suggested by the TG. As indicated in OECD TG 431, RhE tissues (0.5 cm^2, day 17) were transferred into 1 mL maintenance medium in a 6-well plate, and incubated overnight at 37 °C, 5% CO_2 and 95% of humidity. RhE samples were then exposed to 20 mg of each GRM or CBM (40 mg cm^{-2}) for 3 min and 1 h, after adding 20 μL of distilled H_2O, in duplicate. As negative and positive controls, tissues were exposed to distilled H_2O and 8 N potassium hydroxide (KOH), respectively. The tissues were then washed thoroughly 20 times with 1 mL PBS and transferred into each well of a 24-well plate containing 300 μL of MTT solution (1 mg mL^{-1}). The plate was then incubated for 3 h at 37 °C, 5% CO_2 and 95% humidity. Formazan salts were extracted from both the top and bottom sides of each tissue insert with 1.5 mL isopropanol, for 2 h under gentle shaking at RT. The tissues were than perforated and the formazan extract was homogenized. For each tissue, 200 μL of this solution were transferred into each well of a 96-well plate, in triplicate, and isopropanol was used as a blank. Tissue viability was evaluated in terms of formazan concentration, measuring the OD of each extract at 570 nm using the FLUOstar® Omega microplate reader (BMG LABTECH; Ortenberg, Germany). After subtracting the blank OD from all raw data, the mean OD and standard error were calculated. The results of tissue viability are reported as % of negative controls (vehicle) and are the mean ± SE of three independent experiments. As thresholds given by OECD TG 431, skin corrosion was predicted by one of the following parameters: (i) viability <50% after 3 min exposure or (ii) viabilities ≥50% after 3 min exposure and <15% after 1 h exposure (Table 1).

Statistical analysis

The results on skin corrosion and irritation (OECD TG 431 and 439, respectively) are expressed as the % of viability with respect to the negative control, and are the mean ± SE of three experiments performed in duplicate. Statistical analysis was performed by a one-way analysis of variance (ANOVA) followed by Bonferroni's post-test (GraphPad Prism version 8.0); statistical significance was considered for p values <0.05. Heatmap and hierarchical clustering analyses for inflammatory mediators were performed using the R software (version 4.1.2).

Table 1 Prediction model for the SkinEthic™ RhE skin corrosion test method, associated with the UN GHS classification system[30]

Viability measured after exposure time points (3 and 60 min)	Prediction to be considered
Step 1	
<50% after 3 min exposure	Corrosive (C)
≥50% after 3 min exposure AND <15% after 60 min exposure	Corrosive (C)
≥50% after 3 min exposure AND ≥15% after 60 min exposure	Non-corrosive (NC)
Step 2 for substances identified as corrosive in step 1	
<18% after 3 min exposure	Optional sub-category 1A
≥18% after 3 min exposure	Optional sub-category 1B and 1C

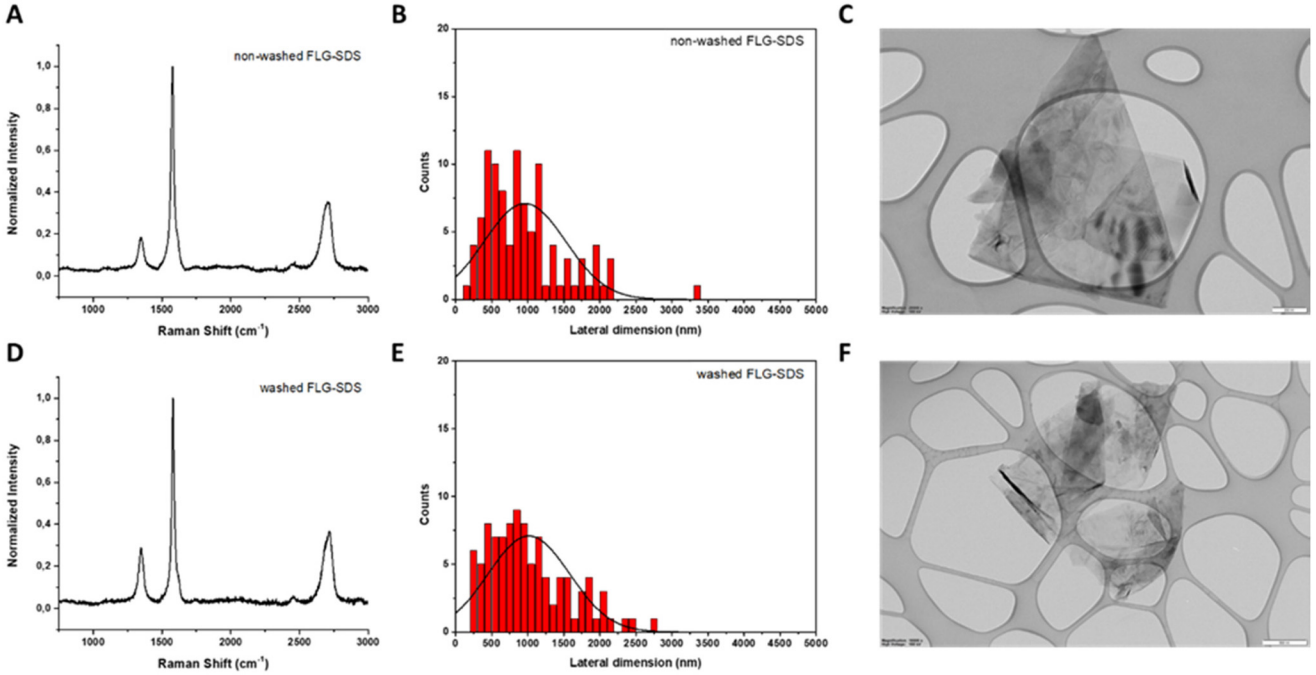

Fig. 1 Physico-chemical characterization of non-washed FLG-SDS (A, B and C) and washed FLG-SDS (D, E and F). (A and D) Raman spectra; (B and E) lateral dimension distribution; and (C and F) representative TEM image. Scale bar: 200 nm (C) and 500 nm (F).

Results

Characterization of GRMs

Non-washed and washed FLG-SDS. Both materials were characterized by Raman spectroscopy, TEM, TGA and elemental analysis. Raman spectroscopy allows us to obtain structural information about the prepared materials, such as the number of layers or the presence of defects.[31] In the non-washed and washed FLG-SDS spectra, the three characteristic peaks of graphitic materials (D, G and 2D bands) are clearly observed (Fig. 1, panels A and D).

The number of layers can be determined from the change of intensity and position of the 2D band (~2700 cm^{-1}): 4 layers were calculated for non-washed FLG-SDS and 6 layers for washed FLG-SDS.[32] In addition, the intensity ratio between the D (~1350 cm^{-1}) and G (~1580 cm^{-1}) bands, $I(D)/I(G)$, allows us to evaluate the number of defects. Being 0.18 in the non-washed material and 0.28 for the washed one, these values suggest low levels of defects.

The lateral dimensions of both materials were estimated by TEM analysis after the measurement of 100 different sheets for each.

The lateral size distribution was located between 150 and 3350 nm with an average lateral dimension of 956 ± 553 nm for non-washed FLG-SDS (Fig. 1, panel B) and between 250 and 2750 nm with an average lateral dimension of 1016 ± 564 nm for washed FLG-SDS (Fig. 1, panel E). Representative TEM images are shown in Fig. 1.

Thermogravimetric analyses (TGA) were carried out to determine the amount of SDS present in the exfoliated materials after the synthetic procedure. As can be seen in the curves, the bulk graphite does not exhibit a significant weight loss (1%) (Fig. 2, panel A). Taking this into account, the weight loss observed in the as prepared FLG materials is due to the

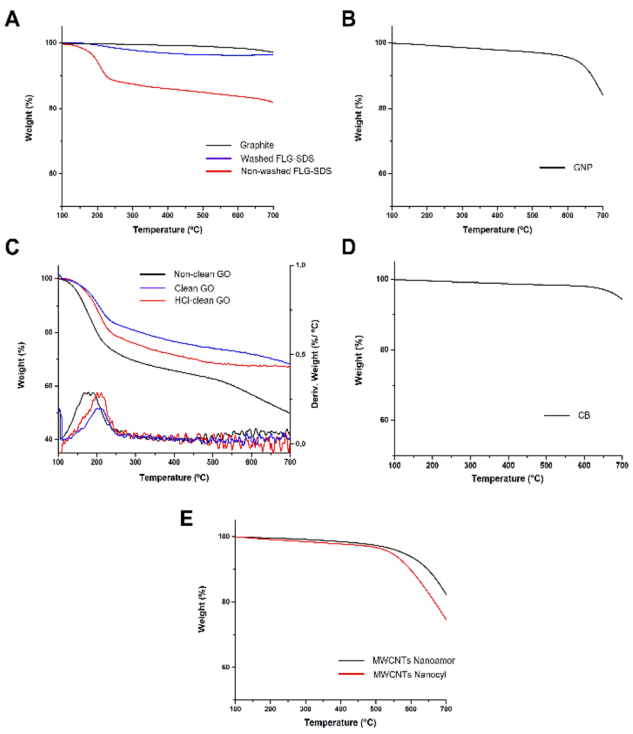

Fig. 2 Thermogravimetric analyses (TGA) of non-washed FLG-SDS and washed FLG-SDS (A), GNP (B), research-grade GO (C), CB (D) and MWCNTs NanoAmor and Nanocyl (E).

presence of the surfactant. In fact, the weight loss for washed FLG-SDS (4% at 600 °C) is significantly lower than the one determined for non-washed FLG-SDS (16% at 600 °C), confirming the successful removal of the surfactant. These results are compatible with the quantity of SDS calculated from elemental analysis (1.4 mg and 41.6 mg of SDS in 100 mg of washed and non-washed FLG-SDS, respectively; Table 2).

GNP. In this case, in addition to the above-mentioned characterization techniques, GNP was subjected to ICP/MS analysis to determine the possible presence of metals. As in the two previous GRMs, Raman spectroscopy was performed to determine the number of layers, and it was calculated as 3 layers for GNP.[32] In this case, the $I(D)/I(G)$ ratio value was 0.29 (Fig. 3, panel A).

TEM analysis was conducted to assess the lateral dimensions of GNP. After the evaluation of 100 different sheets, it was found that the lateral size distribution was centered between 270 and 4500 nm with an average lateral dimension of 1360 ± 695 nm (Fig. 3, panels B and C).

In the TGA curve (Fig. 2, panel B), a weight loss of 4% at 600 °C was noticed, indicating a low quantity of oxygenated groups in the material. This result was corroborated by the slight oxygen content determined by elemental analysis (less than 3.06%; Table 2). In addition, ICP/MS analyses revealed a Fe concentration of 1.734 mg L^{-1} (ESI Table 2†).

Research-grade GO. With the aim to determine the influence of different impurities that can be present in GO not properly purified, three GO samples with diverse cleaning degrees were prepared (non-clean GO, HCl-clean GO and clean GO). These three GRMs were characterized by Raman and X-ray diffraction (XRD) spectroscopy, TEM, TGA, elemental and ICP/MS analyses.

In the case of GO, Raman spectroscopy allows us to detect in a fast and simple way if the oxidation of bulk graphite was successful, since significant changes in its Raman spectrum can be noticed.[33] An intense D band arises as a consequence of high defect concentration introduced by the oxidative treatment. Besides, the intensity of the 2D band decreases and splits.[34] All these features were observed in the Raman spectra of non-clean GO (Fig. 4, panel A), HCl-clean GO (Fig. 4, panel D) and clean GO (Fig. 4, panel G).

Since the 2D band of GO is not well-defined in its Raman spectrum, the number of layers of this GRM was determined by XRD spectroscopy. For this purpose, the characteristic peak of GO, corresponding to its (002) plane, located at 2θ = 10.9°–11.9°, was used to calculate the interlayer space and subsequently the number of layers of the three as-prepared GO[35] (see ESI, Fig. S1† for calculation details). For non-clean GO, the analysis of the XRD spectrum revealed 7 layers. In the case of HCl-clean GO and clean-GO, the number of layers was 5 for both (ESI Fig. S1†).

The lateral dimensions of these materials were estimated by TEM analysis after the measurement of 100 different sheets for each case. The lateral size distribution was located between 60 and 9210 nm with an average lateral dimension of 1204 ± 1638 nm for non-clean GO (Fig. 4, panels B and C), between 150 and 10 700 nm with an average lateral dimension of 2415 ± 2173 nm for HCl-clean GO (Fig. 4, panels E and F) and between 490 and 8700 nm with an average lateral dimension of 2350 ± 1521 nm for clean-GO (Fig. 4, panels H and I).

TGA was accomplished to corroborate the oxidation of graphite and to follow the purification procedure (Fig. 2, panel C). As observed in the Raman spectrum of GO, the first derivative of its TGA curve presents a distinctive peak in a specific

Table 2 Elemental analysis of GBMs and CBMs

	Elemental analysis (%)				
	C	H	N	S	O
Non-washed FLG-SDS	49.62	1.93	0.12	4.63	<43.70
Washed FLG-SDS	65.54	0.75	0	0.16	<33.55
GNP	96.40	0.24	0.14	0.16	<3.06
Non-clean GO	44.30	2.51	0.13	3.25	<49.81
HCl-clean GO	51.18	2.18	0.16	1.05	<45.43
Clean GO	55.13	2.07	0.23	1.35	<41.22
GO[a]	59.40	1.40	0.07	2.50	<36.6
rGO[a]	81.30	0.82	0.21	0	<17.7
Carbon black	98.35	0.17	0.11	0.46	<0.91
MWCNTs NanoAmor	96.13	0.19	0.20	0	<3.48
MWCNTs Nanocyl	94.89	0.52	0.15	0.14	<4.30

[a] For a complete physico-chemical characterization refer to Fusco *et al.* (2020).[25]

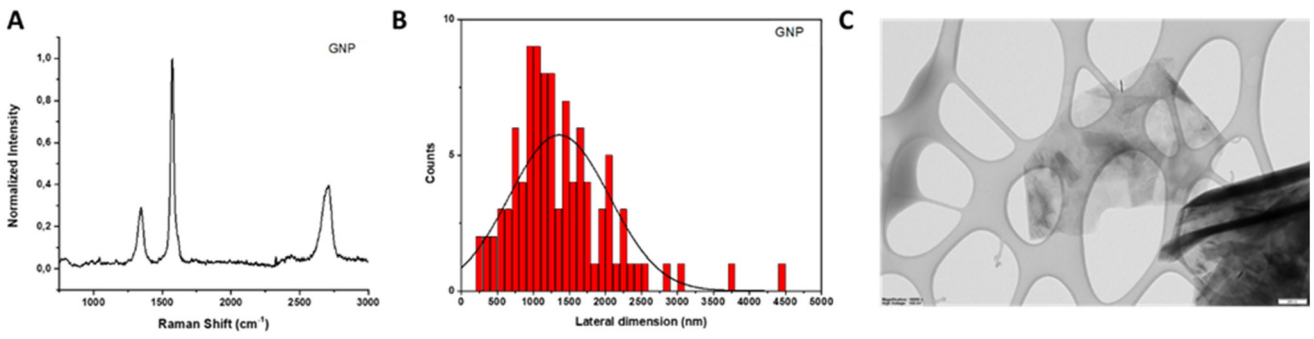

Fig. 3 Physico-chemical characterization of GNP. (A) Raman spectrum; (B) lateral dimension distribution; and (C) representative TEM image. Scale bar: 200 nm.

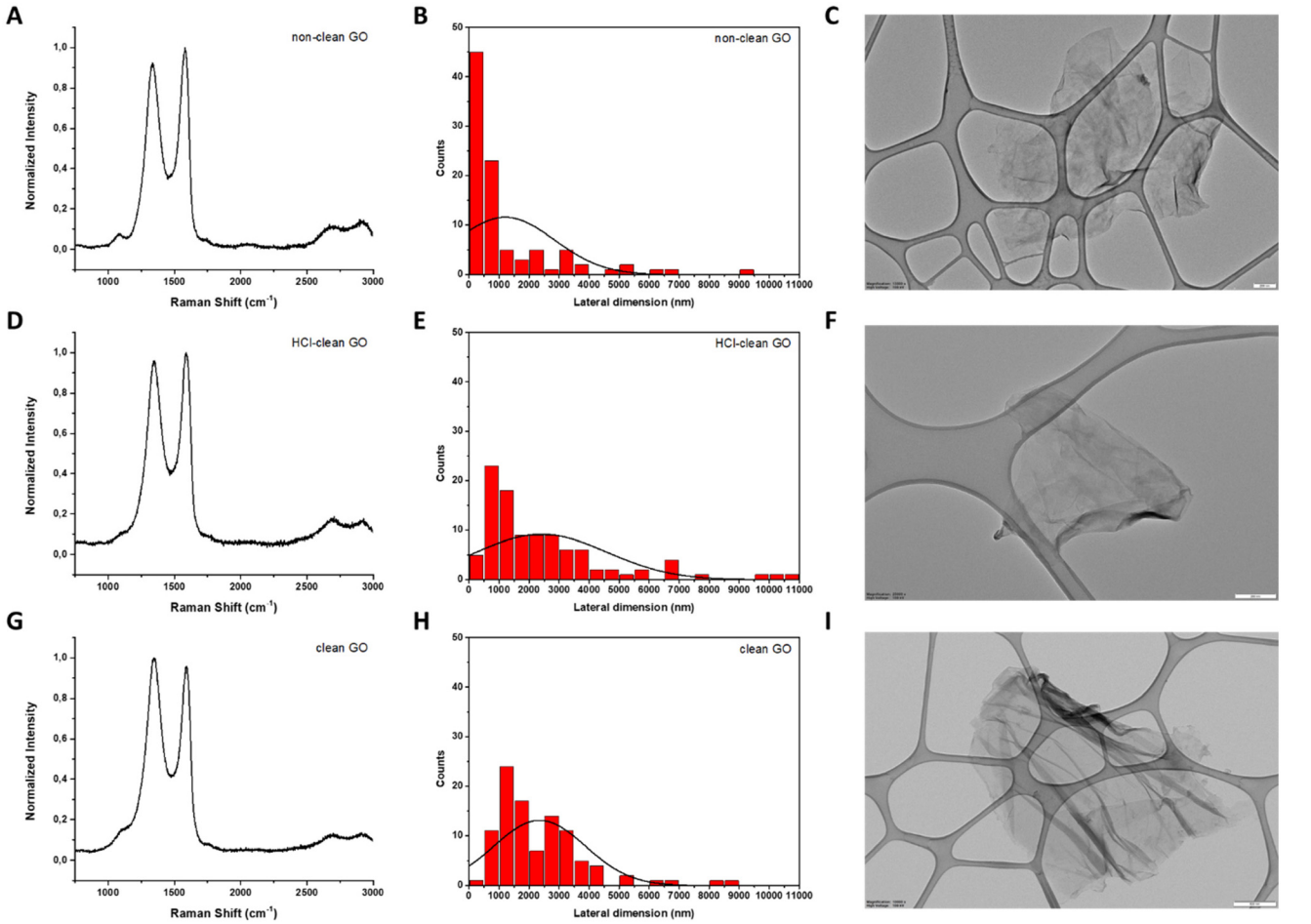

Fig. 4 Physico-chemical characterization of non-clean GO (A, B and C), HCl-clean GO (D, E and F) and clean GO (G, H and I). (A, D and G) Raman spectra. (B, E and H) Lateral dimension distribution. (C, F and I) Representative TEM images. Scale bar: 200 nm (C and F) and 500 nm (I).

range of temperature (T_{max} ~ 180–220 °C) that allows us to distinguish GO from other GRMs.[36] Indeed, this peak is evident in the first derivative curve of the three different GO prepared. In addition, it can be noticed that after each purification step (cleaning with HCl and neutralization with Milli-Q water) the weight loss decreases, being 43% for non-clean GO, 32% for HCl-clean GO and 28% for clean-GO, proving the successive cleaning of the material. These results can be explained by the chemical composition revealed by elemental and ICP/MS analyses. In the first one, it can be noticed that the content of oxygen and sulphur is reduced after each cleaning step due to the removal of the different salts produced during the synthetic procedure (Table 2). A similar trend can be noticed in ICP/MS analysis. The Mn concentration (from the $KMnO_4$ used in the oxidation) diminishes from 1.469 mg L^{-1} in non-clean GO to 0.069 mg L^{-1} in HCl-clean GO and to 0.058 mg L^{-1} in clean GO, corroborating the success of the washing steps (ESI Table T3†).

Characterization of CBMs

Carbon black (CB). CB is composed of aggregates of primary particles with a spherical shape. These particles are in the range of 10–100 nm and contain graphitic and amorphous domains.[37] Their characterization was carried out by Raman and XRD spectroscopy, TEM, TGA, elemental and ICP/MS analyses.

In this case, Raman spectroscopy provides information about the size of the graphitic domains (L_a) and the proportion of amorphous carbon (Fig. 5, panel A). Making use of the empirical formula described by Tuinstra and Koenig ($L_a = 4.35 \frac{I_G}{I_D}$ (nm)), it is possible to evaluate the size of the graphitic domains, obtaining a value of 4.48 nm.[38] The proportion of amorphous carbon can be evaluated by the presence of a broad peak around 1530 cm^{-1} and its relative intensity compared to the G band. This value was calculated as the ratio between the areas of both peaks, equal to 0.86 (ESI Fig. S2, panel A†).

Additional structural information was obtained from XRD analysis, such as the distance between carbon layers and the height of the graphitic domains (L_c).[37] For the CB employed in this study, the distance between layers is 0.353 nm, in the range reported in the literature for other CBs.[39] The value of L_c was estimated using the Debye–Scherrer formula, being 0.99 nm, in agreement with other reported data[39] (ESI Fig. S2, panel B†).

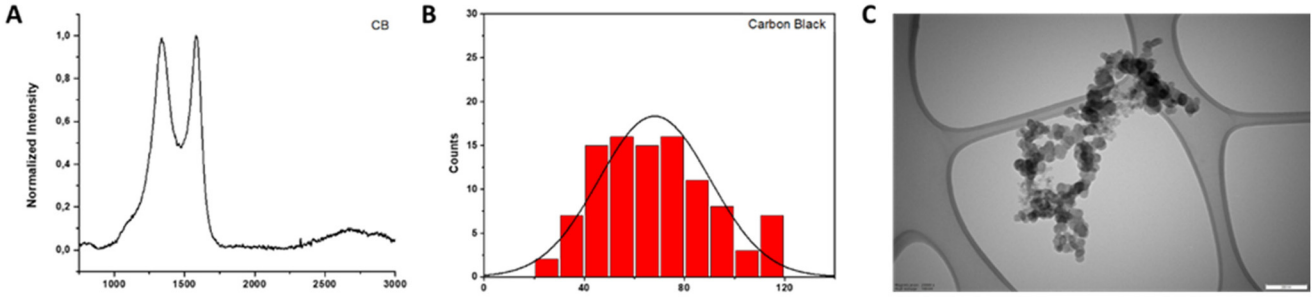

Fig. 5 Physico-chemical characterization of carbon black (CB). (A) Raman spectrum; (B) lateral dimension distribution; and (C) representative TEM image. Scale bar: 200 nm.

TEM analysis was performed with the aim to estimate the lateral dimensions of the material. For this purpose, 100 different particles were evaluated. The lateral size distribution was located between 28 and 118 nm with an average lateral dimension of 68 ± 22 nm (Fig. 5, panels B and C).

In the TGA curve, a weight loss of 2% at 600 °C was noticed, indicating a low quantity of oxygenated groups in the material (Fig. 2, panel D). This result was corroborated by the slight oxygen content determined by elemental analysis (less than 0.91%; Table 2). Besides, ICP/MS analysis was carried out to determine the presence of metals in CB, revealing a very low concentration of Fe and Co (ESI Fig. S2, panel C†).

MWCNTs: NanoAmor and Nanocyl. Two types of MWCNTs, with different diameters, were used in this work. Their characterization was accomplished by Raman spectroscopy, TEM, TGA, elemental and ICP/MS analyses.

In the Raman spectra of both MWCNTs, the three characteristic peaks of graphitic materials are present (Fig. 6, panels A and D). The value of the $I(D)/I(G)$ ratio in NanoAmor MWCNTs is 1.46 and it is 1.49 for Nanocyl MWCNTs.

The MWCNT diameter was assessed by TEM analysis, measuring 100 different MWCNTs for each type. The diameter distribution was located between 14 and 46 nm with an average diameter of 24 ± 6 nm for NanoAmor MWCNTs (Fig. 6, panels B and C) and between 6 and 34 nm with an average diameter of 13 ± 4 nm for Nanocyl MWCNTs (Fig. 6, panels E and F).

The TGA curves showed a weight loss of 6% and 10% for the MWCNTs NanoAmor and Nanocyl, respectively (Fig. 2, panel E). Also in this case, this low value indicates a small quantity of oxygenated groups, as corroborated by elemental analysis (Table 2).

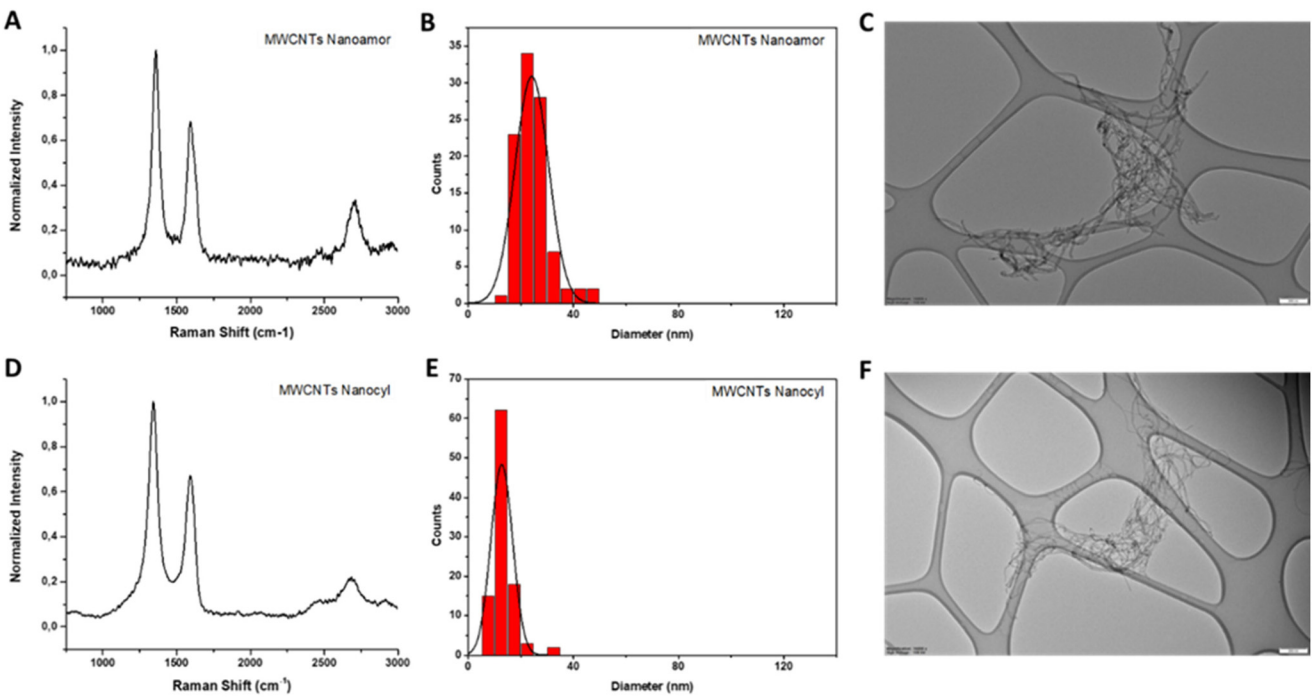

Fig. 6 Physico-chemical characterization of MWCNTs. Raman spectra of MWCNTs NanoAmor (A) and Nanocyl (D); lateral dimension distributions of MWCNTs NanoAmor (B) and Nanocyl (E); representative TEM images of MWCNTs NanoAmor (C) and Nanocyl (F). Scale bar: 200 nm.

Since MWCNTs were employed without further purification, ICP/MS analyses were performed to study the existence of metals derived from the synthesis. These analyses revealed concentrations of 0.443 mg L^{-1}, 0.073 mg L^{-1} and 6.562 mg L^{-1} for Fe, Co and Ni, respectively, in the case of NanoAmor MWCNTs. For Nanocyl MWCNTs, an Fe concentration of 12.787 mg L^{-1} and a Co concentration of 4.099 mg L^{-1} were determined (ESI Table T4†).

Skin irritation. The irritation potential of the selected GRMs was evaluated following the procedure stated in OECD TG 439: after the addition of 10 μL distilled H_2O for tissue wetting, RhE samples were exposed for 42 min to each material (32 mg cm^{-2}, as a powder), and post-incubated for 42 h. Then, MTT assay was carried out to evaluate tissue viability as a parameter for irritation prediction.

Firstly, to assess the suitability of OECD TG 439 for GRMs, two parameters were assessed: (i) the final readout, since GRMs may interfere with the OD measurement of formazan produced by MTT reduction[28] and (ii) materials concentrations, since 32 mg cm^{-2} represents a very high concentration of GRMs, volumetrically speaking, considering their lightweight nature.

For the first parameter, two materials were considered: (i) an irritant GRM, represented by non-washed FLG-SDS, obtained through exfoliation with SDS and (ii) a non-irritant material, represented by washed FLG-SDS, a FLG-SDS sample subjected to washing procedures to remove surfactant residues. Fig. 7 shows the viability of RhE exposed to washed FLG-SDS or non-washed FLG-SDS (0.5–2.0–8.0–32.0 mg cm^{-2}), assessed by the MTT assay in comparison with that measured by the WST-8 assay. Panel A shows RhE viability measured by the MTT assay: only non-washed FLG-SDS induced a significant reduction of tissue viability at levels below the threshold given by the TG to define an irritant substance (≤50%), at concentrations of 8.0 mg cm^{-2} (6.7%, $p < 0.001$) and 32.0 mg cm^{-2} (4.5%, $p < 0.001$). At these concentrations, almost comparable results were obtained by measuring tissue viability by the WST-8 assay (Fig. 7, panel B): non-washed FLG-SDS reduced RhE viability to 8.0% at 8.0 mg cm^{-2} ($p < 0.001$) and 4.2% at 32.0 mg cm^{-2} ($p < 0.001$). In addition, WST-8 assay appeared to overestimate the effect of non-washed FLG-SDS at a concentration of 2.0 mg cm^{-2} (30.3% viability, $p < 0.001$) with respect to the MTT assay (63.8% viability, $p < 0.05$). These results could be due to the already reported higher sensitivity of the WST-8 assay as compared to that of the MTT assay. In contrast, as expected, washed FLG-SDS did not affect tissue viability, evaluated by both assays. Hence, since at GRM concentrations reducing tissue viability at levels predicting skin irritation properties, MTT and WST-8 assays provided comparable results, the substitution of the MTT assay with the WST-8 one appears to be unnecessary.

The results reported in Fig. 7 suggest the possibility to reduce the amount of materials down to 8.0 mg cm^{-2}, the lowest amount of the irritant non-washed FLG-SDS able to reduce RHE viability at a level lower than 50% as the threshold predicting irritation potential. To verify this possibility, the MTT assay was repeated with rGO (0.5–2.0–8.0–32.0 mg cm^{-2}), a mild toxic material for RhE. Fig. 8 shows that rGO induced a significant reduction of RhE viability only at 32.0 mg cm^{-2} (88.8%, $p < 0.05$), at a level above the threshold given by the TG (≤50%). Thus, it can be considered as a non-irritant, but mildly toxic, material for RhE. Nevertheless, rGO at lower amounts (0.5–2.0–8.0 mg cm^{-2}) did not induce any significant alteration of tissue viability. Hence, to assess slightly toxic materials, such as rGO, RhE exposure to amounts reduced up to 8.0 mg cm^{-2} appears unfeasible for evaluating skin irritation since the effects could not predict the real toxicity potential of these materials.

On the basis of the previous results and considerations, OECD TG 439 was followed without any modification to evalu-

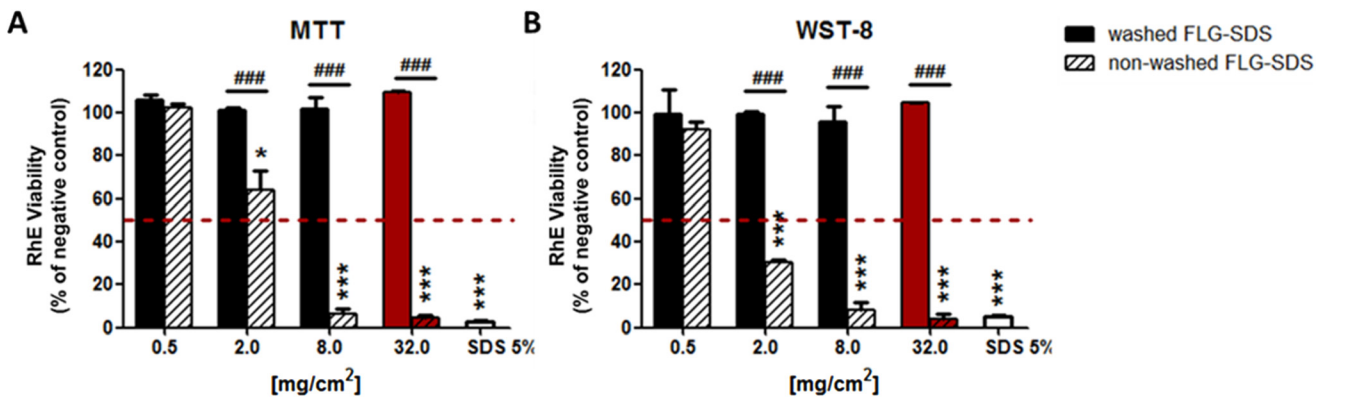

Fig. 7 RhE viability after exposure to washed FLG-SDS, non-washed FLG-SDS or sodium dodecyl sulfate (SDS 5%; positive control) for 42 min, followed by 42 h post-treatment, in compliance with OECD TG 439. Tissue viability was assessed by MTT assay (A) and WST-8 assay (B). Red columns represent the viability of RhE exposed to the materials concentration indicated by OECD TG 439. Data are expressed as % tissue viability with respect to negative controls and are the mean ± SE of three independent experiments. Irritation prediction was defined considering the threshold given by OECD TG 439 (dashed red line). Statistical differences *vs.* negative controls: *, $p < 0.05$; ***, $p < 0.001$; statistical differences (washed FLG-SDS *vs.* non-washed FLG-SDS): ###, $p < 0.001$ (one-way ANOVA and Bonferroni's post-test).

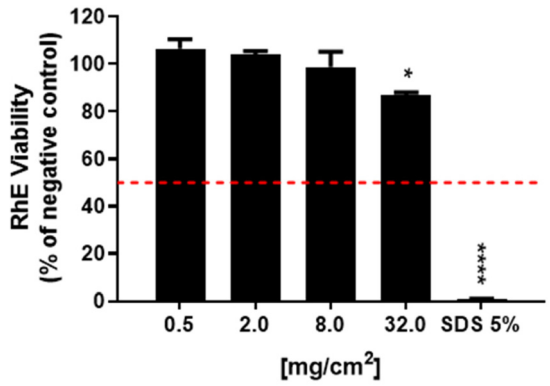

Fig. 8 RhE viability after exposure to rGO or sodium dodecyl sulfate (SDS 5%; positive control) for 42 min, followed by 42 h post-treatment incubation, in compliance with OECD TG 439. Tissue viability was assessed by MTT assay. Data are expressed as % tissue viability with respect to negative controls and are the mean ± SE of three independent experiments. Irritation prediction was defined considering the threshold given by OECD TG 439 (dashed red line). Statistical differences *vs.* negative controls: *, $p < 0.05$; ****, $p < 0.0001$ (one-way ANOVA and Bonferroni's post-test).

ate the irritation properties of a wide panel of GRMs. A set of CBMs, including different types of multiwall carbon-nanotubes (MWCNTs) and carbon black (CB), was added as reference materials.

In Fig. 9, the results show that only non-washed FLG-SDS and the positive control (SDS) significantly decreased tissue viability at 4.5% ($p < 0.0001$) and 1.3% ($p < 0.0001$), respectively. These levels, lower than the threshold predicting skin irritation (≤50%), suggest irritant properties. Moreover, rGO reduced RhE viability at 88.8% ($p < 0.05$), which do not suggest an irritation potential. All the other tested materials did not reduce tissue viability at levels below the threshold given by OECD TG 439 (≤50%), suggesting that they are not skin irritants.

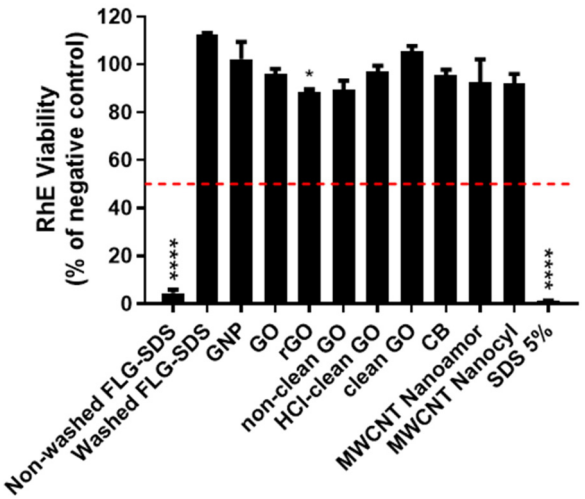

Fig. 9 RhE viability after exposure to GRMs of CBMs (32 mg cm^{-2}) or sodium dodecyl sulfate (SDS 5%; positive control) for 42 min, followed by 42 h post-treatment incubation, in compliance with OECD TG 439. Data are expressed as % tissue viability with respect to negative controls and are the mean ± SE of three independent experiments. Irritation classification was defined on the basis of the threshold given by OECD TG 439 (dashed red line). Statistical differences *vs.* negative controls: *, $p < 0.05$; ****, $p < 0.0001$ (one-way ANOVA and Bonferroni's post-test).

Inflammatory mediators' release

To implement the information given by the application of OECD TG 439, the medium of each RhE tissue exposed to each material (42 min exposure, followed by 42 h post-treatment incubation) was collected. Each medium was analysed quantifying selected inflammatory mediators (IL-1α, −1β, −6, −8, −18, TNF-α and PGE_2) to evaluate GBMs' ability to stimulate epidermal keratinocytes as initiators of a possible skin inflammation. Fig. 10 shows the inflammatory mediators (pg mL^{-1}) released by RhE exposed to GBMs, CBMs or 5% SDS (positive control), in comparison with those by RhE exposed to PBS (negative control).

Regarding IL-1α (Fig. 10, panel A), only non-washed FLG-SDS significantly increased IL-1α release, by 9.7-fold (from 42 pg mL^{-1} of negative control to 406 pg mL^{-1}; $p < 0.0001$). Its effect was significantly higher than that of washed FLG-SDS (63 pg mL^{-1}; $p < 0.001$). SDS (positive control) exerted a comparable effect, inducing a 10.9-fold increase of IL-1α release (458 pg mL^{-1}; $p < 0.0001$). Only non-washed FLG-SDS induced a slight but significant release of IL-6 (1.7-fold increase, from 7 pg mL^{-1} of negative control to 12 pg mL^{-1}; $p < 0.0001$) (Fig. 10, panel C) and IL-8 (2.9-fold increase, from 58 pg mL^{-1} of negative control to 169 pg mL^{-1}; $p < 0.0001$). IL-6 and IL-8 release induced by non-washed FLG-SDS was significantly higher than that induced by washed FLG-SDS (7 pg mL^{-1} IL-6, $p < 0.001$; 67 pg mL^{-1} IL-8, $p < 0.001$). Moreover, IL-8 release induced by non-washed FLG-SDS was higher than that induced by SDS as a positive control (1.9-fold increase, 112 pg mL^{-1}; $p < 0.001$). Also GO determined a slight, but significant, increase of IL-8 release (1.7-fold, 98 pg mL^{-1}; $p < 0.01$) (Fig. 10, panel D). Regarding TNF-α, almost all the tested materials, except non-washed FLG-SDS, caused a slight, but significant, TNF-α release: as compared to negative controls, TNF-α was released at concentrations equal to 30 pg mL^{-1} for GNP ($p < 0.05$), 31 pg mL^{-1} for washed FLG-SDS ($p < 0.01$), non-clean GO ($p < 0.05$), clean GO ($p < 0.01$), CB ($p < 0.01$) and NanoAmor MWCNTs ($p < 0.01$), 32 pg mL^{-1} for GO ($p < 0.0001$), rGO ($p < 0.0001$) and HCl-clean GO ($p < 0.0001$), and 33 pg mL^{-1} for Nanocyl MWCNTs ($p < 0.0001$) (Fig. 10, panel F). In addition, only non-washed FLG-SDS induced a slight PGE_2 release (from 1.6 pg mL^{-1} of negative control to 1.8 pg mL^{-1}; $p < 0.01$), similar to SDS as a positive control (1.8 pg mL^{-1}; $p < 0.05$) (Fig. 10, panel G). In contrast, none of the GBMs or CBMs and SDS influenced the release of IL-1β (Fig. 10, panel B) and IL-18 (Fig. 10, panel E).

Hierarchical cluster analysis was performed to define association dendrograms between the patterns of inflamma-

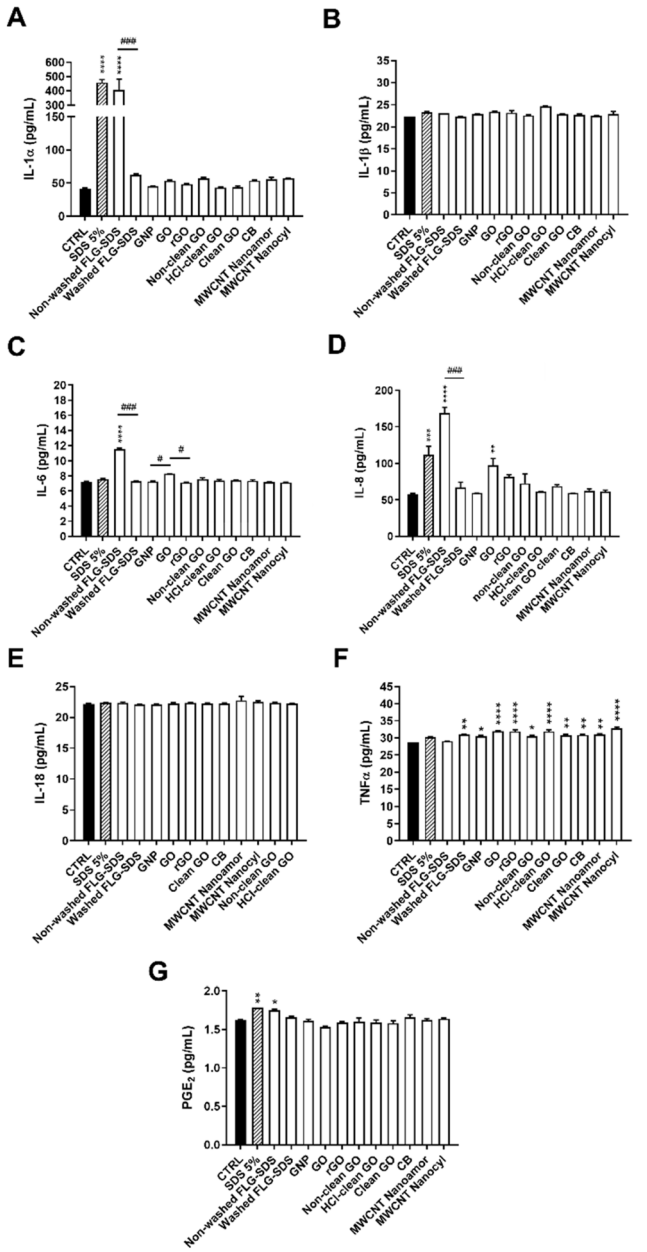

Fig. 10 Inflammatory mediators' release from RhE exposed to GRMs or CBMs for 42 min, followed by 42 h of post-treatment incubation. IL-1α (A), IL-1β (B), IL-6 (C), IL-8 (D), IL-18 (E), TNF-α (F) and PGE_2 (G) were quantified in RhE media by specific ELISA assays. As a positive control, RhE was exposed to 5% SDS. Data, expressed as inflammatory mediators' concentration in the media (pg mL^{-1}), are the mean ± SE of three independent experiments. Statistical differences *vs.* negative controls: *, $p < 0.05$; **, $p < 0.01$; ***, $p < 0.001$; ****, $p < 0.0001$. Statistical differences among materials of the same subgroup: #, $p < 0.05$; ###, $p < 0.001$ (one-way ANOVA and Bonferroni's post-test).

tory mediators' release for each tested material, as presented in Fig. 11. The analysis showed three major clusters: (i) the first comprising non-washed FLG-SDS and the positive control SDS, which suggests a comparable release pattern among the two treatments, supporting the results obtained adopting

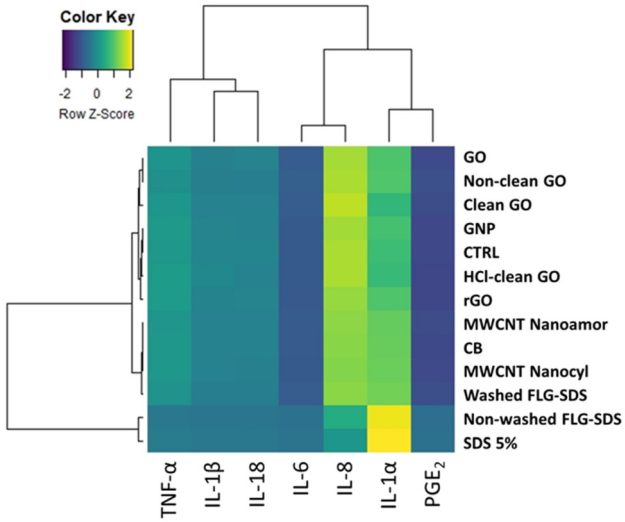

Fig. 11 Hierarchical cluster analysis of inflammatory mediators released by RhE exposed to GRMs or CBMs for 42 min, followed by 42 h of post-treatment incubation. As positive control, RhE was exposed to 5% SDS. Each branch in the dendrograms shows similarity among samples, with shorter branches representing more comparable samples. Association clusters for samples and inflammatory mediators are represented by dendrograms at the left and at the top of the heatmap, respectively.

OECD TG 439; (ii) a second cluster consisting of washed FLG-SDS, CB and the two types of MWCNTs, and (iii) a third one composed of all the other GRMs and negative control, suggesting a very low pro-inflammatory potential of these materials.

Skin corrosion

Considering the similarities between the protocols of OECD TG 439 and 431, the same assumptions to adopt OECD TG 439 for GRMs was made also for the latter. Therefore, skin corrosion was assessed adopting OECD TG 431 without any modification. The corrosion potential of GRMs, and CBMs as reference materials, was evaluated by exposing RhE to 20 mg of each powdered material (40 mg cm^{-2}) for 3 min and 1 h, after wetting with 20 μL distilled H_2O. At the end of each treatment period, RhE viability was evaluated by the MTT assay.

As shown in Fig. 12, none of the GRMs or CBMs tested reduced RhE viability at levels below the threshold defined by OECD TG 431 after 3 min or 1 h exposure (tissue viability <50% after 3 min exposure or <15% after 1 h exposure). Therefore, they can be considered as non-corrosive (NC) materials. However, 1 h treatment with non-washed FLG-SDS significantly reduced RhE viability to 83% ($p < 0.05$), similar to non-clean GO and clean GO that significantly decreased tissue viability at 83% ($p < 0.05$) and 80% ($p < 0.01$), respectively. However, these viability levels are far higher than the threshold defining corrosive properties. In contrast, the positive control (8 N KOH) significantly reduced tissue viability to 3% after

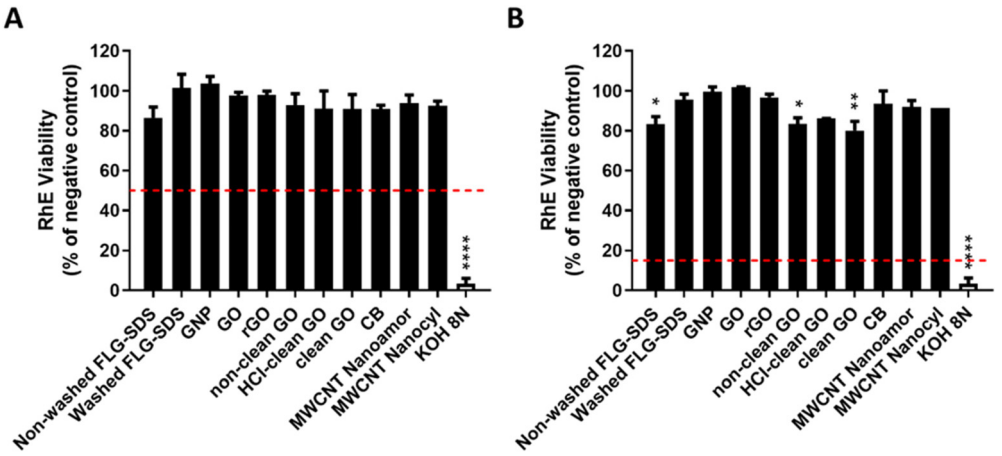

Fig. 12 RhE viability after 3 min (A) or 1 h (B) exposure to GRMs or CBMs (40 mg cm^{-2}), or potassium hydroxide (8N KOH, positive control), in compliance with OECD TG 431. Data are expressed as % of RhE viability with respect to the negative control and are the mean ± SE of three independent experiments. Corrosion classification was defined on the basis of the thresholds given by OECD TG 431, represented by the dashed red lines. Statistical differences *vs.* negative controls: *, $p < 0.05$; **, $p < 0.01$; ****, $p < 0.0001$ (one-way ANOVA and Bonferroni's post-test).

3 minutes treatment ($p < 0.0001$), demonstrating that it is a corrosive (C) substance, as expected.

Discussion

In the last few years, the use of CBMs, in particular GRMs, has widely increased due to their unique physical, chemical, electrical, thermal, mechanical and optical properties. The broad applications of these materials range from electronics, biomedical technologies and energy storage to composites, coatings, water and wastewater treatments.[1,40] Given the wide range of potential uses and considering the entry of GRM-enabled products into the market, the actual risk for human health posed by these materials should be deeply assessed. Until a few years ago, this risk was exclusively correlated with occupational settings, during their industrial or small-scale production. In this context, skin contact and inhalation could be considered the most relevant exposure routes for workers.[3] Nowadays, the development of applications and industrial implementations of GRMs have heavily increased[2] and skin contact could be considered one of the most relevant exposure routes in these situations. Indeed, GRMs can be considered useful nanotools for a wide range of applications at the skin level, such as drug delivery systems, flexible electronics, smart textiles, wound healing dressings, electronic skin and skin sensors.[8–11] Thus, to characterize the hazard posed by these materials at the skin level, several *in vitro* studies have been carried out on fibroblasts and keratinocytes.[12–20]

However, common *in vitro* 2D cell cultures do not appropriately mimic the physiological and morphological features of the skin, including its barrier properties. In this view, 3D models of epidermis are more complete and predictive models. These models have been further developed in compliance with the 3R's principles (replacement, reduction and refinement) aiming at minimizing and optimizing *in vivo* testing.[41] Recently, 3D skin models have been included in the New Approach Methodologies (NAMs) as alternative methods and strategies useful in providing information on hazard and risk assessment of a substance while avoiding the use of animals.[42,43] Furthermore, the potential skin irritation and corrosion are important factors that must be considered in establishing procedures for safe handling, packing and transport of these materials. Indeed, the evaluation of skin irritation and corrosion potential is mandatory for all substances to be placed into the market under international regulatory requirements.[30,44]

Thus, this study was aimed at assessing skin irritation and corrosion properties of GRMs on the SkinEthic™ Reconstructed human Epidermis (RhE), a standardized 3D model of epidermis obtained from human-derived non-transformed keratinocytes, which closely simulates the histological, morphological, biochemical and physiological properties of the upper part of human skin, the epidermis.[24] Using this model, two *in vitro* methods were developed to evaluate skin irritation and corrosion potential of chemical substances.[45,46] These procedures were reported in two specific test guidelines (TGs) given by the Organization for Economic Co-operation and Development (OECD),[27,29] which defines wide commonly accepted processes that should be strictly followed to identify and characterize the hazards of chemicals, allowing us to achieve toxicological data suitable to assess their safety also for regulatory purposes.

In particular, we evaluated the skin irritation and corrosion potential of GRMs, and some CBMs used as reference materials, following OECD TG 439 and 431, respectively. The protocols of the two TGs are similar in terms of model and readout: they predict skin irritation or corrosion potential by means of a reduced tissue viability after treatment with the substances under test, using the well-known MTT assay.

However, these TGs were originally validated for chemicals, even though OCTD TG 439 has been already applied to different kinds of nanomaterials, including polymeric nanoparticles,[47] metal-based nanoparticles[48] and CBMs, such as MWCNTs[49] and a limited panel of GRMs.[25] In particular, despite the latter being previously tested by our group applying OECD TG 439, a complete assessment of the TG suitability without any drawbacks was not performed.[25] Therefore, before enlarging the panel of GRMs to be evaluated for their skin irritation and corrosion properties, an initial step assessing the suitability of the OECD TGs for GRMs was necessary. Given the similarity between the two guidelines, this assessment was carried out for OECD TG 439. In particular, two critical parameters were examined: (i) the final readout, since the MTT reagent could be prone to give unspecific interferences with GRMs[28] and (ii) the amount of materials, since 32 mg GRMs per cm^2 epidermis surface area represents a very high amount in terms of volume, considering their weight–volume ratio and their lightweight nature. Regarding the first point, we compared the results obtained by the MTT assay suggested by the TG with those obtained by the WST-8 assay, an MTT-analogue test not affected by interferences with GRMs.[28] Using a previously defined irritant (non-washed FLG-SDS) and a non-irritant (washed FLG-SDS) GRM,[25] our results demonstrated that the MTT assay can be used to quantify RhE viability, without the need for being substituted by the WST-8 assay. Indeed, no differences in RhE viability were found using the two assays to test GRMs at amounts above 8 mg cm^{-2}, which excludes false negative results by unspecific interactions between the materials and the probe. This finding confirmed our previous observation suggesting that the barrier property of RhE does not allow GRMs deposited on the RhE surface to pass into the compartment below the RhE tissue in which the MTT reagent is added.[25] In addition, the WST-8 assay appeared to slightly overestimate the effect of the irritant non-washed FLG-SDS, at least at 2.0 mg cm^{-2} probably due to its higher sensitivity as compared to that of other tetrazolium dye assays, such as MTT, XTT and MTS.[50] Regarding the second parameter, our results suggest that the amount of GRMs deposited on RhE cannot be lowered since this modification could lead to a wrong prediction of their toxicity potential. Indeed, while prediction of skin irritation appeared accurate for non-irritant and irritant GRMs down to an amount of 8 mg cm^{-2}, this was not observed for a mildly toxic GRM, such as rGO. In fact, 8 mg rGO per cm^2 did not induce any significant effect on RhE, in contrast to the amount recommended by OECD TG 439 (32 mg cm^{-2}) which significantly decreased the tissue viability, even though at levels not predicting skin irritation. Therefore, lowering the deposited amount of GRMs could not allow an accurate discrimination of mildly toxic GRMs, leading to possible misclassifications. Altogether, these findings suggest that OECD TG 439, and by extension also to OECD TG 431 given their similarities, can be adopted for GRMs without the need for protocol changes.

Consequently, we assessed the irritation potential of a wide panel of GRMs, including FLG prepared with a toxic surfactant (FLG-SDS) with or without washings to remove SDS residues, commercially available GO, rGO and GNP as well as a set of research-grade GOs obtained by a modified Hummers' method and characterized by different degrees of oxidation reagent clean-up (clean GO, HCl-clean GO and non-clean GO), the latter included to evaluate the impurities' (*i.e.* chemical reagent residues) influence on skin irritation by GO. Other CBMs, such as CB and two types of MWCNTs, were tested as reference materials. As stated by the TG, skin irritation prediction is based on the ability of the test substance to reduce tissue viability (measured by the MTT assay) at $\leq$50% after 42 min exposure, followed by 42 h of post-treatment RhE incubation.[27] The results showed that, among the panel of tested GRMs, only non-washed FLG-SDS reduced tissue viability at a level lower than the 50% threshold (4.5% tissue viability), suggesting an irritation potential only for this material. In addition, rGO induced a significant reduction of RhE viability (at 88.8%), above the threshold level predicting an irritation effect. Notably, GNP and all the GOs did not affect tissue viability, independent of their clean-up degree. This observation suggests that also GOs obtained by a modified Hummers' method, in which the strong reducing reagents are not sufficiently removed, are non-skin irritants, highlighting their safety for the skin. Similar results were obtained also for the reference CBMs (CB and MWCNTs): none of them significantly reduced RhE viability and, therefore, they can be considered as non-irritant materials, in accordance with previous findings for MWCNTs assessed by OECD TG 439[51] and *in vivo* by the Draize test.[49,51] On the whole, these results demonstrate that GRMs and CBMs are generally not skin irritants, in line with our previous findings showing that only GRMs prepared with specific toxic exfoliation agents (*i.e.* SDS), not sufficiently washed out, are skin irritants, probably due to the high surfactant residues.[25]

Given the pro-inflammatory potential of an irritation response, to implement the information given by OECD TG 439, GBMs and CBMs were evaluated for their ability to stimulate the release of inflammatory mediators by RhE. The quantification of inflammatory mediators can be a useful approach to improve skin irritancy assessment, since an even slight cytotoxicity can act as a stimulus triggering an inflammatory process and even immune stress.[52] For instance, it is well known that the pro-inflammatory cytokine IL-1α, constitutively produced by keratinocytes, can stimulate its own release and the release of other cytokines. Being an important mediator of innate immunity and inflammation, it can be suitable to classify skin irritants using 3D models of epidermis.[53] Accordingly, 5% SDS, used as a positive control for skin irritation as suggested by OECD TG 439, significantly increased IL-1α release by RhE, as previously reported in different studies.[54–57] In a similar way, the irritant FLG-SDS not subjected to washing procedures increased IL-1α release at levels comparable to those induced by the positive control SDS. In contrast, washed FLG-SDS did not affect the cytokine release, indicating that the irritant properties of non-washed FLG-SDS can be ascribed to the surfactant residues in the material.

Similarly, none of the other non-irritant GRMs or CBMs significantly increased IL-1α release, with evidence supporting the lack of irritant properties of these materials. The release of TNF-α, IL-6 and IL-8 was also analysed. All tested materials caused a slight but significant increase of TNF-α secretion, except non-washed FLG-SDS and the positive control SDS. Furthermore, only non-washed FLG-SDS and the commercially available GO induced a moderate release of IL-6 and the chemokine IL-8, two well-known pro-inflammatory cytokines involved in skin inflammation.[58,59] In line with these results, a slight but significant increase of PGE_2 release was found only after RhE treatment with non-washed FLG-SDS or the positive control SDS. Lastly, IL-1β and IL-18, mediators of the acute inflammatory responses providing a link between innate and adaptive immunity,[60] were only barely secreted or not released by RhE exposed to GRMs or CBMs, respectively. IL-18, a biomarker of allergic responses, was evaluated on the basis of literature data demonstrating its suitability to discriminate between irritants and allergens in RhE models.[61] Since none of the tested GRMs, including the irritant FLG-SDS, and CBMs significantly stimulated IL-18 release, our results seem to argue against possible skin sensitization properties of these materials. This observation is line with previous *in vitro* and *in vivo* studies demonstrating that GRMs (FLG, GO and GNP)[23,62] and MWCNTs (Nikkiso-MWCNTs, Mitsui-7 MWCNTs, and low-carboxylated MWCNTs)[63–65] are not skin sensitizers. Anyway, on the whole, the analysis of inflammatory mediators' release by RhE suggests a general low pro-inflammatory potential for both GRMs and CBMs, given the low amounts measured. Only non-washed FLG-SDS appeared to be the highest inflammogenic material; indeed, the clustering analysis on pro-inflammatory mediators' release data defined a first high-affinity cluster of association, comprising non-washed FLG-SDS and the positive control SDS, which suggests a comparable release pattern between the two treatments, driven mainly by the irritation biomarker IL-1α. In addition, it should be also noted that, beside slight differences among GO, rGO and GNP in inducing IL-6 release, major significant differences related to inflammatory mediator (IL-1α, IL-6, and IL-8) release were observed only between non-washed and washed FLG-SDS, confirming that the washing procedure not only neutralized the irritation potential of non-washed FLG-SDS, but also reduced its pro-inflammatory properties.

In the second part of the study, the same panel of GRMs and CBMs was tested for their skin corrosion potential, referred to as the induction of an irreversible skin damage, namely necrosis of the epidermis after its exposure to a substance. The method defined by OECD TG 431 is based on the premise that a corrosive substance can penetrate the *Stratum corneum* of epidermis by diffusion or erosion and it might be cytotoxic to cells in the underlying layers.[29,30] The method compliant with OECD TG 431 was set up and chosen as the best for its high reproducibility, accuracy and predictive capability.[29] Corrosion prediction is based on the ability of substances to reduce tissue viability (measured by the MTT assay) at levels <50% after 3 min exposure and <15% after 1 h exposure. Given the similarity of OECD TG 431 to OECD TG 439 in terms of tissue model, exposure conditions and readout, the same considerations made to adopt the latter for GRMs was extended also to assess skin corrosion. Hence, TG 431 was adopted for GRMs, and CBMs as reference materials, without any modification of the procedure. The results showed that none of the tested materials reduced tissue viability at levels lower than those predicting skin corrosion. Only 1 h treatment with non-washed FLG-SDS significantly reduced tissue viability to 83%, at a level higher than the threshold given by the TG. A comparable effect was exerted also by non-clean GO and clean GO, which significantly decreased RhE viability at 83% and 80%, respectively. Therefore, it can be underlined that, not only GRMs, but also the irritant non-washed FLG-SDS appears to be non-corrosive, despite its high surfactant residues. Similarly, non-clean GO (potentially containing a strong acid derived from the oxidation process of graphite) and HCl-clean GO (potentially containing traces of corrosive HCl) turned out to be non-corrosive for the skin. In addition, to the best of our knowledge, no data on skin corrosion are currently available for CBMs, tested as reference materials, which for the first time suggests that also MWCNTs and CB are not skin corrosive.

Conclusions

In conclusion, this study has successfully adopted OECD TG 439 and 431 to assess the skin irritation and corrosion properties of GRMs, respectively, without any required modification of the procedures. It should be acknowledged that the ToxRTool[66] was used to classify our study following the principles of the Klimisch score (K score), providing comprehensive criteria and guidance for reliability evaluations of toxicological data.[67,68] The present study resulted in a score of 17 out of 18, indicating that it is in Klimisch category 1 (reliable without restrictions), therefore highlighting the reliability of the data. In general, the results of our study suggest that a wide panel of different GRMs (including FLG exfoliated with SDS, commercially available GO, rGO and GNP, and a set of research-grade GOs characterized by different clean-up degrees) as well as reference CBMs (MWCNTs and CB) can be considered as non-irritant and non-corrosive materials. Only FLG exfoliated with the toxic surfactant SDS, not sufficiently removed from the final product, demonstrated irritant but not corrosive properties, confirming the hypothesis that the irritation potential can be ascribed to the surfactant residues in the final material. Anyway, despite the general low inflammogenic potential of the tested materials, the slight but significant release of some inflammatory cytokines (IL-1α, IL-6, IL-8, and TNF-α) induced by a few GRMs, in particular non-washed FLG-SDS, raises some concerns. Indeed, the findings using this 3D RhE model do not rule out a possible involvement of other immune-competent cells, such as neutrophils, or Langerhans' cells as the antigen-presenting cells of the skin. Thus, the use of other advanced models, more predictive of

immune-based cutaneous outcomes, would be useful to extend the knowledge on the adverse effects of GRMs at the skin level.

Author contributions

M. Carlin: investigation and writing – original draft; M. Garrido: resources, investigation, and writing – original draft; S. Sosa: data curation, formal analysis, and writing – review & editing; A. Tubaro: writing – review & editing; M. Prato: funding acquisition, project administration, and writing – review & editing; M. Pelin: conceptualization, supervision, and writing – review & editing.

Conflicts of interest

There are no conflicts to declare.

Acknowledgements

This study was financially supported by the European Commission Graphene Flagship Core 3 (grant agreement no. 881603). This work was partly developed under the Maria de Maeztu Units of Excellence Program from the Spanish State Research Agency (Grant No. MDM-2017-0720).

References

1 T. Sattar, *Top. Curr. Chem.*, 2019, **377**, 10.
2 R. and M. ltd, *Graphene Market Size, Share & Trends Analysis Report by Material (Graphene Oxide, Graphene Nanoplatelets), by Application (Electronics, Composites), by Region (APAC, Europe), and Segment Forecasts, 2021-2028*, **https://www.researchandmarkets.com/reports/4751759/graphene-market-size-share-and-trends-analysis**.
3 M. Pelin, S. Sosa, M. Prato and A. Tubaro, *Nanoscale*, 2018, **10**, 15894–15903.
4 R. and M. ltd, *The Graphene Market, Production and Pricing Report 2022*, **https://www.researchandmarkets.com/reports/5548353/the-graphene-market-production-and-pricing**.
5 Registration Dossier - ECHA, **https://echa.europa.eu/it/registration-dossier/-/registered-dossier/24678**.
6 Understanding REACH - ECHA, **https://echa.europa.eu/regulations/reach/understanding-reach**.
7 B. Fadeel, C. Bussy, S. Merino, E. Vázquez, E. Flahaut, F. Mouchet, L. Evariste, L. Gauthier, A. J. Koivisto, U. Vogel, C. Martín, L. G. Delogu, T. Buerki-Thurnherr, P. Wick, D. Beloin-Saint-Pierre, R. Hischier, M. Pelin, F. Candotto Carniel, M. Tretiach, F. Cesca, F. Benfenati, D. Scaini, L. Ballerini, K. Kostarelos, M. Prato and A. Bianco, *ACS Nano*, 2018, **12**, 10582–10620.
8 N. Karim, S. Afroj, D. Leech and A. M. Abdelkader, *Oxide Electronics*, John Wiley & Sons, Ltd, 2021, pp. 21–49.
9 S. Syama and P. V. Mohanan, *Nano-Micro Lett.*, 2019, **11**, 6.
10 S. R. Shin, Y.-C. Li, H. L. Jang, P. Khoshakhlagh, M. Akbari, A. Nasajpour, Y. S. Zhang, A. Tamayol and A. Khademhosseini, *Adv. Drug Delivery Rev.*, 2016, **105**, 255–274.
11 Y.-Q. Liu, Z.-D. Chen, J.-W. Mao, D.-D. Han and X. Sun, *Front. Chem.*, 2019, **7**, 461.
12 Y. Li, H. Yuan, A. von dem Bussche, M. Creighton, R. H. Hurt, A. B. Kane and H. Gao, *Proc. Natl. Acad. Sci. U. S. A.*, 2013, **110**, 12295–12300.
13 M. Pelin, L. Fusco, V. León, C. Martín, A. Criado, S. Sosa, E. Vázquez, A. Tubaro and M. Prato, *Sci. Rep.*, 2017, **7**, 40572.
14 M. Pelin, L. Fusco, C. Martín, S. Sosa, J. Frontiñán-Rubio, J. M. González-Domínguez, M. Durán-Prado, E. Vázquez, M. Prato and A. Tubaro, *Nanoscale*, 2018, **10**, 11820–11830.
15 J. Frontiñán-Rubio, M. V. Gómez, C. Martín, J. M. González-Domínguez, M. Durán-Prado and E. Vázquez, *Nanoscale*, 2018, **10**, 11604–11615.
16 B. Salesa, A. Tuñón-Molina, A. Cano-Vicent, M. Assis, J. Andrés and Á. Serrano-Aroca, *Appl. Sci.*, 2022, **12**, 720.
17 M. Pelin, H. Lin, A. Gazzi, S. Sosa, C. Ponti, A. Ortega, A. Zurutuza, E. Vázquez, M. Prato, A. Tubaro and A. Bianco, *Nanomaterials*, 2020, **10**, 1602.
18 T. Pulingam, K. L. Thong, J. N. Appaturi, C. W. Lai and B. F. Leo, *Chemosphere*, 2021, **281**, 130739.
19 J. Frontiñan-Rubio, M. V. Gomez, V. J. González, M. Durán-Prado and E. Vázquez, *Sci. Rep.*, 2020, **10**, 18407.
20 A. Dalla Colletta, M. Pelin, S. Sosa, L. Fusco, M. Prato and A. Tubaro, *Carbon*, 2022, **196**, 683–698.
21 L. Fusco, M. Pelin, S. Mukherjee, S. Keshavan, S. Sosa, C. Martín, V. González, E. Vázquez, M. Prato, B. Fadeel and A. Tubaro, *Carbon*, 2020, **159**, 598–610.
22 H. Kim, J. Choi, H. Lee, J. Park, B.-I. Yoon, S. M. Jin and K. Park, *Toxicol. Res.*, 2016, **32**, 311–316.
23 S. Sosa, A. Tubaro, M. Carlin, C. Ponti, E. Vázquez, M. Prato and M. Pelin, *NanoImpact*, 2023, **29**, 100448.
24 F. Netzlaff, C.-M. Lehr, P. W. Wertz and U. F. Schaefer, *Eur. J. Pharm. Biopharm.*, 2005, **60**, 167–178.
25 L. Fusco, M. Garrido, C. Martín, S. Sosa, C. Ponti, A. Centeno, B. Alonso, A. Zurutuza, E. Vázquez, A. Tubaro, M. Prato and M. Pelin, *Nanoscale*, 2020, **12**, 610–622.
26 D. C. Marcano, D. V. Kosynkin, J. M. Berlin, A. Sinitskii, Z. Sun, A. Slesarev, L. B. Alemany, W. Lu and J. M. Tour, *ACS Nano*, 2010, **4**, 4806–4814.
27 OECD, *Test No. 439: In Vitro Skin Irritation: Reconstructed Human Epidermis Test Method*, Organisation for Economic Co-operation and Development, Paris, 2021.
28 K.-H. Liao, Y.-S. Lin, C. W. Macosko and C. L. Haynes, *ACS Appl. Mater. Interfaces*, 2011, **3**, 2607–2615.
29 OECD, *Test No. 431: In vitro skin corrosion: reconstructed human epidermis (RHE) test method*, Organisation for Economic Co-operation and Development, Paris, 2019.
30 *Globally harmonized system of classification and labelling of chemicals (GHS)*, ed. V. Nationen, United Nations, New York, Geneva, 2021.

31 A. C. Ferrari, J. C. Meyer, V. Scardaci, C. Casiraghi, M. Lazzeri, F. Mauri, S. Piscanec, D. Jiang, K. S. Novoselov, S. Roth and A. K. Geim, *Phys. Rev. Lett.*, 2006, **97**, 187401.
32 K. R. Paton, E. Varrla, C. Backes, R. J. Smith, U. Khan, A. O'Neill, C. Boland, M. Lotya, O. M. Istrate, P. King, T. Higgins, S. Barwich, P. May, P. Puczkarski, I. Ahmed, M. Moebius, H. Pettersson, E. Long, J. Coelho, S. E. O'Brien, E. K. McGuire, B. M. Sanchez, G. S. Duesberg, N. McEvoy, T. J. Pennycook, C. Downing, A. Crossley, V. Nicolosi and J. N. Coleman, *Nat. Mater.*, 2014, **13**, 624–630.
33 D. López-Díaz, M. López Holgado, J. L. García-Fierro and M. M. Velázquez, *J. Phys. Chem. C*, 2017, **121**, 20489–20497.
34 S. Claramunt, A. Varea, D. López-Díaz, M. M. Velázquez, A. Cornet and A. Cirera, *J. Phys. Chem. C*, 2015, **119**, 10123–10129.
35 D. Torres, D. Sebastián, M. J. Lázaro, J. L. Pinilla, I. Suelves, A. S. Aricò and V. Baglio, *Electrochim. Acta*, 2019, **306**, 396–406.
36 F. Farivar, P. L. Yap, K. Hassan, T. T. Tung, D. N. H. Tran, A. J. Pollard and D. Losic, *Carbon*, 2021, **179**, 505–513.
37 M. Pawlyta, J.-N. Rouzaud and S. Duber, *Carbon*, 2015, **84**, 479–490.
38 T. Ungár, J. Gubicza, G. Ribárik, C. Pantea and T. W. Zerda, *Carbon*, 2002, **40**, 929–937.
39 A. Cuesta, P. Dhamelincourt, J. Laureyns, A. Martínez-Alonso and J. M. D. Tascón, *Carbon*, 1994, **32**, 1523–1532.
40 J. Li, H. Zeng, Z. Zeng, Y. Zeng and T. Xie, *ACS Biomater. Sci. Eng.*, 2021, **7**, 5363–5396.
41 C. Riebeling, A. Luch and T. Tralau, *Exp. Dermatol.*, 2018, **27**, 526–536.
42 A. J. van der Zalm, J. Barroso, P. Browne, W. Casey, J. Gordon, T. R. Henry, N. C. Kleinstreuer, A. B. Lowit, M. Perron and A. J. Clippinger, *Arch. Toxicol.*, 2022, **96**, 2865–2879.
43 F. Pistollato, F. Madia, R. Corvi, S. Munn, E. Grignard, A. Paini, A. Worth, A. Bal-Price, P. Prieto, S. Casati, E. Berggren, S. K. Bopp and V. Zuang, *Arch. Toxicol.*, 2021, **95**, 1867–1897.
44 C. Eskes, V. Detappe, H. Koëter, J. Kreysa, M. Liebsch, V. Zuang, P. Amcoff, J. Barroso, J. Cotovio, R. Guest, M. Hermann, S. Hoffmann, P. Masson, N. Alépée, L. A. Arce, B. Brüschweiler, T. Catone, R. Cihak, J. Clouzeau, F. D'Abrosca, C. Delveaux, J. P. Derouette, O. Engelking, D. Facchini, M. Fröhlicher, M. Hofmann, N. Hopf, J. Molinari, A. Oberli, M. Ott, R. Peter, V. M. Sá-Rocha, D. Schenk, C. Tomicic, P. Vanparys, B. Verdon, T. Wallenhorst, G. C. Winkler and O. Depallens, *Regul. Toxicol. Pharmacol.*, 2012, **62**, 393–403.
45 C. Tornier, M. Roquet and A. de B. de Fraissinette, *Toxicol. in Vitro*, 2010, **24**, 1379–1385.
46 N. Alépée, C. Tornier, C. Robert, C. Amsellem, M.-H. Roux, O. Doucet, J. Pachot, M. Méloni and A. de B. Fraissinette, *Toxicol. in Vitro*, 2010, **24**, 257–266.
47 R. Bengalli, L. Fiandra, C. Vineis, D. O. Sanchez-Ramirez, N. G. Azoia, A. Varesano and P. Mantecca, *Nanomaterials*, 2021, **11**, 1991.
48 R. Bengalli, A. Colantuoni, I. Perelshtein, A. Gedanken, M. Collini, P. Mantecca and L. Fiandra, *NanoImpact*, 2021, **21**, 100282.
49 A. S. Kishore, P. Surekha and P. B. Murthy, *Toxicol. Lett.*, 2009, **191**, 268–274.
50 H. Tominaga, M. Ishiyama, F. Ohseto, K. Sasamoto, T. Hamamoto, K. Suzuki and M. Watanabe, *Anal. Commun.*, 1999, **36**, 47–50.
51 Y.-H. Park, S. H. Jeong, E. Y. Lee, S.-H. Lee, B. H. Choi, M.-K. Kim and S. W. Son, *Toxicol. Environ. Health Sci.*, 2010, **2**, 115–118.
52 M. Pasparakis, I. Haase and F. O. Nestle, *Nat. Rev. Immunol.*, 2014, **14**, 289–301.
53 E. Corsini and C. L. Galli, *Toxicol. Lett.*, 1998, **102–103**, 277–282.
54 S. W. Spiekstra, M. J. Toebak, S. Sampat-Sardjoepersad, P. J. van Beek, D. M. Boorsma, T. J. Stoof, B. M. E. von Blomberg, R. J. Scheper, D. P. Bruynzeel, T. Rustemeyer and S. Gibbs, *Exp. Dermatol.*, 2005, **14**, 109–116.
55 C. Pellevoisin, C. Videau, D. Briotet, C. Grégoire, C. Tornier, A. Alonso, A. S. Rigaudeau, C. Bouez and N. Seyler, *Toxicol. in Vitro*, 2018, **50**, 418–425.
56 V. Martinez, E. Corsini, M. Mitjans, A. Pinazo and M. P. Vinardell, *Toxicol. Lett.*, 2006, **164**, 259–267.
57 D. A. Kidd, M. Johnson and J. Clements, *Toxicol. in Vitro*, 2007, **21**, 1292–1297.
58 M. Baggiolini, B. Dewald and B. Moser, in *Advances in Immunology*, ed. F. J. Dixon, Academic Press, 1993, vol. 55, pp. 97–179.
59 T. Hirano, *Clin. Immunol. Immunopathol.*, 1992, **62**, S60–S65.
60 H. Watanabe, O. Gaide, V. Pétrilli, F. Martinon, E. Contassot, S. Roques, J. A. Kummer, J. Tschopp and L. E. French, *J. Invest. Dermatol.*, 2007, **127**, 1956–1963.
61 E. Corsini, M. Mitjans, V. Galbiati, L. Lucchi, C. L. Galli and M. Marinovich, *Toxicol. in Vitro*, 2009, **23**, 789–796.
62 S.-H. Kim, S.-H. Hong, J. H. Lee, D. H. Lee, K. Jung, J.-Y. Yang, H.-S. Shin, J. Lee, J. Jeong and J.-H. Oh, *Toxics*, 2021, **9**, 62.
63 M. Ema, A. Matsuda, N. Kobayashi, M. Naya and J. Nakanishi, *Regul. Toxicol. Pharmacol.*, 2011, **61**, 276–281.
64 B. C. Palmer, S. J. Phelan-Dickenson and L. A. DeLouise, *Part. Fibre Toxicol.*, 2019, **16**, 3.
65 S.-H. Kim, D. H. Lee, J. H. Lee, J.-Y. Yang, H.-S. Shin, J. Lee, K. Jung, J. Jeong, J.-H. Oh and J. K. Lee, *Toxics*, 2020, **8**, 122.
66 ToxRTool - Toxicological data reliability assessment tool, **https://joint-research-centre.ec.europa.eu/scientific-tools-and-databases/toxrtool-toxicological-data-reliability-assessment-tool_en**.
67 K. Schneider, M. Schwarz, I. Burkholder, A. Kopp-Schneider, L. Edler, A. Kinsner-Ovaskainen, T. Hartung and S. Hoffmann, *Toxicol. Lett.*, 2009, **189**, 138–144.
68 M. L. Fernández-Cruz, D. Hernández-Moreno, J. Catalán, R. K. Cross, H. Stockmann-Juvala, J. Cabellos, V. R. Lopes, M. Matzke, N. Ferraz, J. J. Izquierdo, J. M. Navas, M. Park, C. Svendsen and G. Janer, *Environ. Sci.: Nano*, 2018, **5**, 381–397.